

148

RESEARCH RELATIVE TO HIGH RESOLUTION CAMERA ON THE
ADVANCED X-RAY ASTROPHYSICS FACILITY

Grant NAG8-527

IN-29073

FINAL REPORT

For the Period May 13, 1985, Through March 15, 1986

(NASA-CR-179757) RESEARCH RELATIVE TO HIGH RESOLUTION CAMERA ON THE ADVANCED X-RAY ASTROPHYSICS FACILITY Final Report, 13 May 1985 - 15 Mar. 1986 (Smithsonian Astrophysical Observatory) 14 p CSCL 14E G3/35 44237 N87-10376 Unclas

September, 1986

Prepared for

National Aeronautics and Space Administration
George C. Marshall Space Flight Center
Marshall Space Flight Center, Alabama 35812

Smithsonian Institution
Astrophysical Observatory
Cambridge, Massachusetts 02138

The Smithsonian Astrophysical Observatory
is a Member of the
Harvard-Smithsonian Center for Astrophysics

RESEARCH RELATIVE TO HIGH RESOLUTION CAMERA ON THE
ADVANCED X-RAY ASTROPHYSICS FACILITY

Grant NAG8-527

FINAL REPORT

For the Period May 13, 1985, Through March 15, 1986

Principal Investigator

Stephen S. Murray
Dr. Stephen S. Murray

Associate Director, High Energy Astrophysics Division

Harvey D. Tananbaum
Dr. Harvey D. Tananbaum

September, 1986

Prepared for

National Aeronautics and Space Administration
George C. Marshall Space Flight Center
Marshall Space Flight Center, Alabama 35812

Smithsonian Institution
Astrophysical Observatory
Cambridge, Massachusetts 02138

The Smithsonian Astrophysical Observatory
is a Member of the
Harvard-Smithsonian Center for Astrophysics

I. Introduction

The work described herein was supported under NASA Grant NAG8-527, issued May 1985. This grant was intended primarily to insure continuity of effort in the development of the High Resolution Camera (HRC), pending initiation of a Phase B Contract to support Design Definition activities.

The HRC is one of four experiments selected under NASA AO No. 055A-3-83, Advanced X-ray Astrophysics Facility (AXAF), August 15, 1983. The scientific objectives of the AXAF are clearly specified in the AO and will therefore not be repeated here. The experiment proposed, including the development of the HRC instrument, is fully compliant with the requirements of the AO, and with the Program Requirements Document (PRD).

The work accomplished under this grant is primarily an extension of the Phase A definition initiated earlier under SR&T funding. Therefore, the effort was concentrated on refining concepts for achieving improved resolution, higher sensitivity, and enhanced performance in the HRC alternate operating mode, i.e., as a readout for the objective grating. Minimal effort was expended in addressing the interface requirements of the two different instrument accommodation concepts, or in developing programmatic controls or documentation. For this reason, the work accomplished under this grant is conveniently summarized in the recent paper authored by the P.I., and Project Scientist, Drs. S. Murray and J. Chappell respectively. This paper is reproduced in Section II of this report. In Section III, we present the modified Statement of Work (SOW) to be accomplished during Phase B. The changes to the SOW presented in our original proposal are the result of the additional insight into the requirement of the AXAF instruments, gained during this grant effort, as well as recent funding and schedule changes in the AXAF program.

II. Technical Summary

The following paper appeared in SPIE Vol. 597 X-Ray Instrumentation in Astronomy (1985) journal.

The Advanced X-Ray Astrophysics Facility High Resolution Camera

Stephen S. Murray and Jon H. Chappell

Smithsonian Astrophysical Observatory, 60 Garden Street Mail Stop 6, Cambridge MA 02138

Abstract

The HRC (High Resolution Camera) is a photon counting instrument to be flown on the Advanced X-Ray Astrophysics Facility (AXAF). It is a large field of view, high angular resolution, detector for the x-ray telescope. The HRC consists of a CsI coated microchannel plate (MCP) acting as a soft x-ray photocathode, followed by a second MCP for high electronic gain. The MCPs are readout by a crossed grid of resistively coupled wires to provide high spatial resolution along with timing and pulse height data. The instrument will be used in two modes, as a direct imaging detector with a limiting sensitivity of 10^{-15} ergs/cm² sec in a 10^3 second exposure, and as a readout for an objective transmission grating providing spectral resolution of several hundreds to thousands.

Introduction

The next major x-ray observatory planned by NASA is the Advanced X-Ray Astrophysics Facility (AXAF), for which there was a recent Announcement of Opportunity ⁽¹⁾ for instruments. Among the four instruments selected for Phase B design definition study is the High Resolution Camera (HRC). This is a photon counting detector which provides high resolution images of celestial x-ray sources along with precise information on photon arrival times, and low resolution spectral data.

The AXAF is intended to be a long lived major observatory with a lifetime in excess of 15 years. It will be launched sometime in the 1990's and will carry a 10 meter focal length x-ray telescope consisting of six pairs of nested Wolter Type I mirrors. The telescope will have on axis angular resolution of about 0.5 arc-seconds, and will operate over the energy band from 0.1 to 10 keV. In addition to the HRC, the observatory will include a low energy transmission grating spectrometer (LETGS) that is read out using the HRC. There are two higher energy transmission gratings and three other focal plane instruments that were also selected for Phase B study. These are discussed in companion papers presented at this conference.

The overall scientific objectives of AXAF are ⁽¹⁾:

- .To determine the nature of celestial objects from normal stars to quasars.
- .To understand the nature of physical processes which take place in and between astronomical objects.
- .To understand the history and evolution of the Universe.

The HRC will be used to address these general areas of research. Some of the specific scientific investigations that can be carried out are studies of:

- .The nature and origin of the cosmic x-ray background and the relative contributions of quasars, primordial galaxies, and diffuse gas at cosmological epochs.
- .The nature and origin of nuclear activity in galaxies and quasars, and the physical relationships between AGNs and their host galaxies.
- .The structure and evolution of galaxy clusters and superclusters as probes of the formation of galaxies and theories of the early universe.
- .The mass and nature of haloes of galaxies as derived from observations of the hot gas they contain and from the x-ray properties of stars.
- .The origin of stellar activity as manifested in the x-ray emission from winds and coronae of stars.

These scientific studies require the high angular resolution made possible by the x-ray optics of AXAF and the imaging performance of the HRC. They also require the use of the grating spectrometer to obtain high spectral resolution data for various classes of x-ray sources.

Instrument Description

The HRC is a single photon counter, that is it detects individual x-rays and provides the position, energy, and time of arrival for each. The detector is based on the use of microchannel plates and an electronic readout. It is similar to the highly successful HEAO-2 (Einstein Observatory) High Resolution Imaging Detector (HRI) ^(2,3) which operated

flawlessly for 2½ years in-orbit. The main detector properties are summarized in table 1., they include high spatial resolution and high time resolution over the entire field of view, low internal background, low sensitivity to cosmic ray induced background, high x-ray quantum efficiency from 0.1 to 8 keV, and modest energy resolution particularly at low energies. Compared to the Einstein HRI, the AXAF HRC has substantially increased capability in the areas of quantum efficiency, detector size, reduced background rate, and intrinsic energy resolution. These properties of the HRC, combined with the large area of the AXAF x-ray optics lead to an increase in point source sensitivity of 50 compared with the Einstein HRI. The low background of the HRC also provides a sensitive detector for studies of diffuse sources. The high efficiency and high spatial resolution of the HRC at low x-ray energies allows it to be used as an efficient readout for the grating spectrometer, particularly below 0.5 keV.

The x-ray detector, shown schematically in figure 1, consists of a protective UV/Ion shield; a photocathode, which converts the incident photons to electrons; a set of microchannel plates (MCPs), which amplify the electron signal while maintaining high spatial and temporal resolution; and electronic read out, which uses resistively coupled crossed wire grids (CGCD); and an active plastic scintillator anticoincidence shield, which reduces the induced cosmic ray background. The entire instrument includes two detector assemblies which are housed in a vacuum chamber with calibration and checkout mechanisms such as a UV calibration system, radioactive x-ray sources, and fiducial lights. Electronics providing low voltage power, high voltage bias, event processing, command decoding, and telemetry are also part of the instrument.

The HRC has two principal operating modes, as a direct imaging device and as a readout for the objective grating. In the imaging mode, a single detector assembly is active and the center of the detector is nominally at the axis of the x-ray telescope. In the spectroscopy mode, there are several possible combinations of operating detectors and telescope axis positions. The nominal configuration will be with both detector assemblies active, and the telescope axis position offset to the interior corner of a detector. The detectors are oriented to provide maximal spectral coverage in both first order images from the grating. The low energy grating dispersion is such that in this configuration wavelengths shortward of ~140Å will fall on the detectors. The two detector assemblies are slightly tilted with respect to one another (~30 arc-minutes). This approximates the Rowland circle of the grating and maximizes the energy resolution at the longest wavelengths. Focus adjustments are also provided since the optimal axial position differs in the imaging and spectroscopy modes.

The Instrument Principal Investigator (IPI) team for developing the HRC includes members of the Harvard-Smithsonian Center for Astrophysics, Leicester University, and the University of Hawaii. Overall direction of the project is through the Principal Investigator (PI) at the Smithsonian Astrophysical Observatory (SAO). In the Phase B design definition portion of the project, major responsibilities for detector study have been spread out among the participating organizations to take advantage of the expertise available. Specifically, photocathode and MCP studies are being jointly carried out at SAO and Leicester, UV/Ion shield design is being done at Hawaii, and the readout system and active anticoincidence are being developed at SAO.

Instrument Development

Each of the major detector elements contributes to the overall performance of the HRC. The window determines the low energy efficiency of the detector while providing shielding against ultraviolet radiation and low energy ions which would otherwise dominate the instrument background. The photocathode determines the quantum efficiency, uniformity of response, and energy resolution. We have selected CsI for the photocathode based on the work of Fraser et al. ⁽⁴⁾ who have demonstrated many of the desired properties of a soft x-ray photocathode. The microchannel plates determine the limiting spatial resolution due to their pore size. The operating voltages on the MCPs effect the gain uniformity of the detector, the internal background, and the spectral resolution. The crossed grid charge detector readout also determines the spatial resolution of the HRC, particularly important parameters are the wire and resistor uniformity, and the operating voltages.

Photocathodes

The use of CsI as a soft x-ray photocathode has been discussed by Fraser et al. ⁽⁴⁾, who have measured various properties of CsI deposited directly onto a microchannel plate. Their latest results are described elsewhere in these proceedings ⁽⁵⁾. Chappell et al. have evaporated up to 26,000 Å of CsI onto the front surface of an MCP ⁽⁶⁾ and have confirmed the efficiencies reported by Fraser. The strong dependence of coated MCP detector quantum efficiency on the angle of incidence ⁽⁷⁾ requires the deposition geometry to be optimized for the particular application. In the case of AXAF, the cone angle of the telescope beam ranges from 2° to 4°, and the plate must be coated at angles at least this shallow to insure adequate penetration of the CsI into the channels. The coating process must also be uniform and cylindrically symmetric to insure that there will not be

systematic variations in efficiency or gain. This requires carefully controlled conditions in the deposition process such as rotation of the MCP with respect to the CsI source and sufficient source to MCP distance to insure uniform illumination. In figure 2, the quantum efficiency versus energy is shown for the HRC. This curve is based on theoretical calculations by Fraser⁽⁸⁾ and normalized by measured values at several energies. The effects due to absorption edges in Cs, I, and the MCP glass are included. (9) In addition to the high detection efficiency afforded by the use of CsI, Fraser et al. have shown that it is possible to operate CsI coated MCPs in a mode whereby energy resolution is obtained. Figure 3 shows an example of the pulse height distributions obtained at two different energies using a CsI coated MCP. Fraser and colleagues present more recent results on this aspect of coated channel plates in their contribution to these proceedings⁽⁵⁾.

We have investigated alternatives to directly coating MCPs with x-ray photocathodes. Henke and Henry⁽¹⁰⁾ suggested that free standing cathodes made by depositing low density ("fluffy") CsI on thin plastic films could yield high quantum efficiencies, particularly at energies above 6 keV. We constructed this type of photocathode by evaporating CsI onto stretched polypropylene in a chamber filled with nitrogen at low pressure. The resulting photocathode was placed in front of an MCP chevron and operated at various voltages with respect to the front channel plate. The quantum efficiencies measured were not significantly higher than those for the deposited photocathodes. Moreover, at low energies the window absorption resulted in lower net efficiency when compared with directly deposited cathodes.

We also examined the energy resolution performance of the fluffy photocathode and found that there was no measurable difference in pulse height distributions as function of x-ray energy. This is because the fluffy photocathode produces a secondary electron distribution that peaks at one electron independent of the incident energy⁽¹¹⁾. Only the tail of the distribution changes with energy, and this effect is washed out by the MCP gain characteristic. In the case of deposited CsI photocathodes, the most probable number of secondary electrons depends on incident energy and thus provides energy resolution⁽⁹⁾. The secondary electron yield from CsI deposited onto the MCP increases with increasing x-ray energy. However, the depth of penetration of the x-ray photon also increases with energy so that the most probable number of electrons that escape into the MCP channel to begin the multiplication process does not grow linearly. Measured performance indicates that useful spectral resolution can be obtained only for x-ray energies below about 2 keV.

Microchannel Plates

The microchannel plates we have been using for the HRC are manufactured by Mullard Ltd in the United Kingdom. These are 100mm x 100mm square plates with 12½ µm pores on 15 µm centers. The plates have a length to diameter (l/d) ratio of 120/1, and were specially manufactured for this application. We have also been using somewhat more standard 36mm diameter MCPs from Mullard for our deposition and quantum efficiency measurements. Tests with the large area plates have been limited to imaging studies and background measurements. When we are able to obtain additional large area plates, we will carry out coating tests and lifetime studies to confirm the results from the smaller plates. Since the MCPs are made from the same glass and go through similar processing as the standard Mullard MCPs, we do not anticipate any significant performance changes. We note however, that the background rate in the one set of large area plates we have tested is substantially lower than that of any set of MCPs we have previously measured. This low internal background significantly improves the overall detector performance in terms of signal to noise and sensitivity to low surface brightness objects. We are currently investigating the reasons for such low count rates in a joint program with our colleagues at Leicester University.

The imaging performance of the HRC is demonstrated in figure 4. Here we show an x-ray shadowgraph obtained with the large area MCPs that were illuminated through a mask made from 5 µm thick nickel. The readout used is a 75mm x 75mm CGCD connected to a HEAO-2 event processor. As shown in the figure, the detector can easily resolve the smallest slit pattern on the mask corresponding to 20 lp/mm. An analysis of the image, assuming a gaussian point response function for the detector, results in a measured spatial resolution characterized by FWHM = 25 µm (= 10.6 µm). The resolution obtained is limited mainly by MCP pore size with a small contribution due to electronic noise.

We have recently had discussions with Mullard regarding the availability of large area MCPs with smaller pore size. There appear to be no technical problems with manufacturing them in the HRC format, however at this time there has been no official quotation from Mullard for prices or delivery schedule. The potential advantages of such plates are discussed by Fraser et al.⁽⁵⁾ in terms of improved spectral resolution and lower background. Based on the imaging results discussed above, we predict that MCPs with 8 µm pores would yield spatial resolution characterized by a FWHM of 20µm. Fraser et al.⁽⁵⁾ have shown that the smaller pore size MCPs can be successfully coated with CsI and that they yield improved pulse height distributions.

Read Out System

The crossed grid charge detector (CGCD) used for the Einstein HRI has been described in the literature (3,12). We have constructed two larger readouts which provide 75mm x 75mm active area for imaging studies. The imaging data discussed above was obtained with one of these CGCDs. The data show that the coarse/fine position determination algorithm can be scaled from the 25mm unit with no loss in resolution.

The Einstein HRI readout system used 17 preamplifiers per axis to divide the image plane into 16 x 16 coarse position elements. In the case of the HRC we will have 65 preamplifiers per axis and 64 x 64 coarse image elements. The fine position is determined from a centroid calculation of the charge collected on the grid wires. The precise algorithm to be used for the HRC is one of the areas of investigation during Phase B. For Einstein a 'three tap' calculation was carried out using an analog divide circuit and a multiplying ADC (12). For the HRC we are considering the use of a digital processor and a 'four tap' algorithm. The advantages of this approach are faster event processing time and less systematic distortion in the calculated position. To allow a more complete evaluation of this design, we have built a set of prototype processing electronics which are interfaced to a MASSCOMP MCS-500 computer system. The electronics provide the coarse position encoding and digitization of signals from the CGCD. The computer is used to carry out the fine position calculation which can be modified via software so that a number of algorithms can be studied. The MASSCOMP also serves as the ground support system for the HRC providing command, status, and imaging display capabilities.

Background

The sensitivity of MCPs to high energy charged particles and gamma rays is a major contributor to the total background in detectors such as the HRC. In order to minimize this background source we have designed the instrument with a plastic scintillator shield. Laboratory measurements show that between 50% and 85% of cosmic ray muons produce events in the HRC. Because the HRC is a photon counting detector, it is possible to reject cosmic ray induced events using an anticoincidence system. The resolving time of the HRC is fast (10µsec), and the total count rate from cosmic rays is low (< 100 ct sec⁻¹). The HRC will process all events and include the status of the shield so that the induced events can be screened out during ground processing. Measurements of the pulse height distribution from shields similar to the one planned for the HRC show that more than 99% of all minimum ionizing particles can be detected (13) and thus this component of background effectively reduced.

The background due to gamma rays and compton scattered electrons is not reduced by the anticoincidence system. However, the HRC is relatively insensitive to gamma rays as demonstrated by the observation that the background rate for the Einstein HRC did not increase significantly in orbit over the ground rate. We have measured the response of a chevron MCP detector to gamma rays from 60 keV to 400 keV using radioactive sources. For gamma rays that pass through the plates in the plane normal to the channel axis (the maximum amount of material), there is about a 3% chance of an interaction which is independent of the gamma ray energy in the region studied. Most of these interactions are single compton scattered electrons that are knocked out from the channel walls. These electrons produce low amplitude events in the MCP first because they are single electrons initially, and second because most events occur part way down the channels resulting in less gain. By setting the valid event threshold high enough most of these events are not processed.

Instrument Performance

The predicted performance of the HRC depends upon the performance of the individual elements of the instrument as described above, and the manner in which the AXAF spacecraft and x-ray telescope perform. The baseline AXAF mirror areas are given in the Announcement of Opportunity. Based on the recent measurements from the Test Mirror Assembly (TMA) (14), the expected mirror scattering function and figure have been revised (favorably). We have taken a surface roughness of 10Å and a FWHM of <0.5 arc-seconds to characterize the mirror. Image quality also depends on the precision of the aspect solution obtained. We have assumed that the total on axis point response function will have FWHM <1.0 arc-seconds. In calculating the HRC sensitivity, we included the effects of a 3000Å thick Lexan UV/Ion shield overcoated with 500Å of aluminum. The CsI quantum efficiency shown in figure 2 was assumed.

The detector background is derived from three components, the internal MCP noise, cosmic and gamma ray induced events, and diffuse x-rays. The contributions of these components are listed in table 2. The internal MCP background rate is that measured in the laboratory for HRC type plates as discussed above. The cosmic ray rate assumes a 99% rejection efficiency using an anticoincidence shield. The diffuse x-ray background is based on a model consisting of three parts: a thermal galactic component with temperature 10⁵ °K, emission measure 1.5 x 10⁻⁵ cm⁻³ pc, Hydrogen column 1 x 10²¹ cm⁻²; a second thermal galactic component with temperature 10⁶ °K, emission measure 3.6 x 10⁻⁶ cm⁻³ pc, Hydrogen column 1 x 10²¹ cm⁻²; and a power law extragalactic component of the form

$10E-1.4$ photons $cm^{-2}s^{-1}keV^{-1}ster^{-1}$ with a hydrogen of column density $3 \times 10^{20} cm^{-2}$. The emission measures and Hydrogen column densities used are typical for high galactic latitudes.

Based on these inputs and assumptions, we have calculated the HRC sensitivity for on axis point sources and diffuse sources of 20 arc-second extent. Figure 6 is a plot of a typical sensitivity calculation showing the minimum detectable source flux as a function of observation time. In this figure, the criteria for detectability is that the source flux be measured with a 5 statistical precision (20% measurement error). The source spectrum was taken to be a power law with photon index 1.4 and with a hydrogen column of $3 \times 10^{20} cm^{-2}$.

Acknowledgements

We would like to thank G.K.Austin and J.J.Gomes for their valuable engineering talents, and Dr. R.Rosner for helpful discussions regarding the HRC.

This work was supported by NASA Grant NAG8-527.

References

1. NASA Announcement of Opportunity AO No. OSSA-3-83 Advanced X-Ray Astrophysics Facility, August 15, 1983
2. Giacconni et al., Ap.J. (Letters) Vol. 230 (1979) pp. 540
3. Henry, J.P., Kellogg, E.M., Briel, U.G., Murray, S.S., VanSpeybroeck, L.P., and Bjorkholm, P.J., Proc. SPIE Vol. 106 (1977) pp. 163
4. Fraser, G.W. and Pearson, J.F., Nucl. Instr. Meth. Vol. 219, (1984) pp. 199
5. Fraser, G.W., Whiteley, M.J., and Pearson, J.F., "Developments in Microchannel Plate Detectors for Imaging X-ray Astronomy", these proceedings.
6. Chappell, J.H., Everman, D.E., and Murray, S.S., in preparation
7. Bjorkholm, P.J., VanSpeybroeck, L.P., and Hecht, M. Proc. SPIE Vol. 106 (1977) pp. 189
8. Fraser, G.W. Private Communication (1985)
9. Fraser, G.W., Barstow, M.A., Pearson, J.F., Whiteley, M.J., and Lewis, M., Nucl. Instr. Meth. Vol. 224, (1984) pp. 272
10. Henke, B.L. and Henery, J.P., Private Communication (1983)
11. Garwin, E.L., and Llacer, J., J. Appl. Phys. Vol. 41 (1970) pp. 1489
12. Kellogg, E.M., Henry, J.P., Murray, S.S., VanSpeybroeck, L.P., and Bjorkholm, P.J., Rev. Sci. Instr. Vol. 47, (1976) pp. 282
13. Grindlay, J.E., Garcia, M.A., Burg, R.I., and Murray, S.S., IEEE Trans. Nucl. Sci (1986) to be published
14. Schwartz, D.A., et al. "X-Ray Testing of the AXAF Technology Mirror Assembly (TMA) Mirror" these proceedings

Figure Captions

Figure 1. Schematic Diagram of the AXAF HRC showing the major functional elements.

Figure 2. Quantum detection efficiency of the HRC versus x-ray energy.

Figure 3. Sample pulse height distributions from a CsI coated MCP at two incident energies (taken from Fraser et al ⁽⁹⁾).

Figure 4. An example of HRC imaging performance. X-ray image through a shadow mask plate directly in front of the detector and illuminated with low energy x-rays from a continuum source.

Figure 5. The sensitivity of the HRC as a function of exposure time for point-like and extended sources.

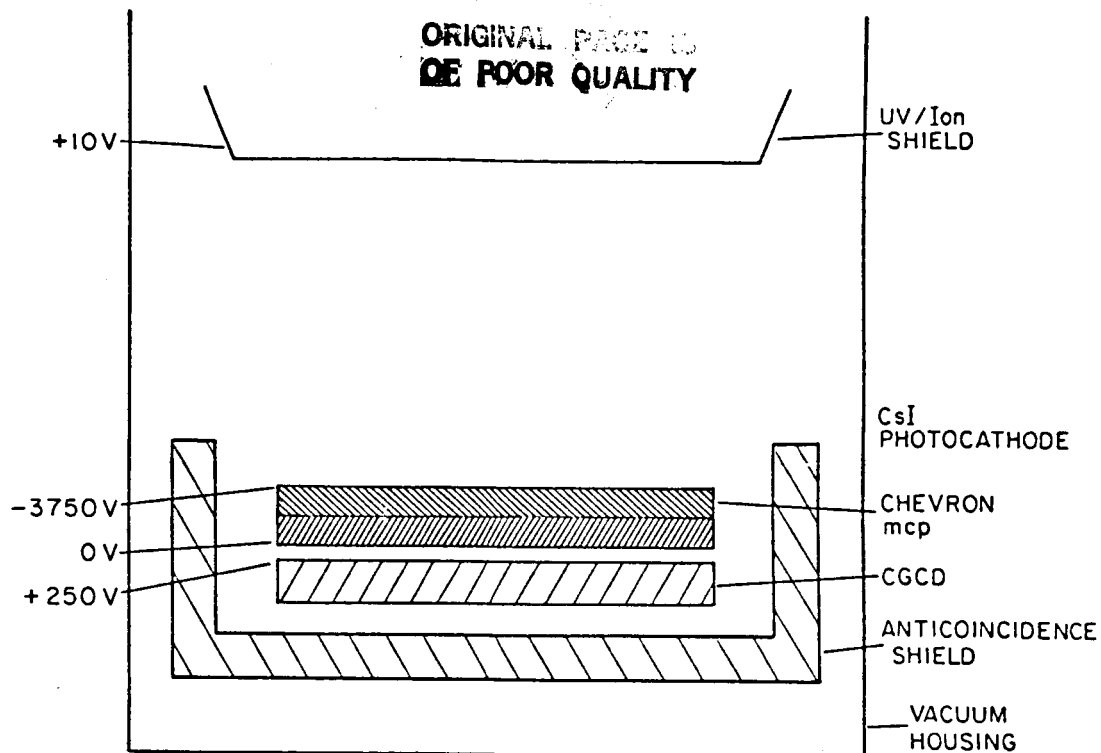


Figure 1

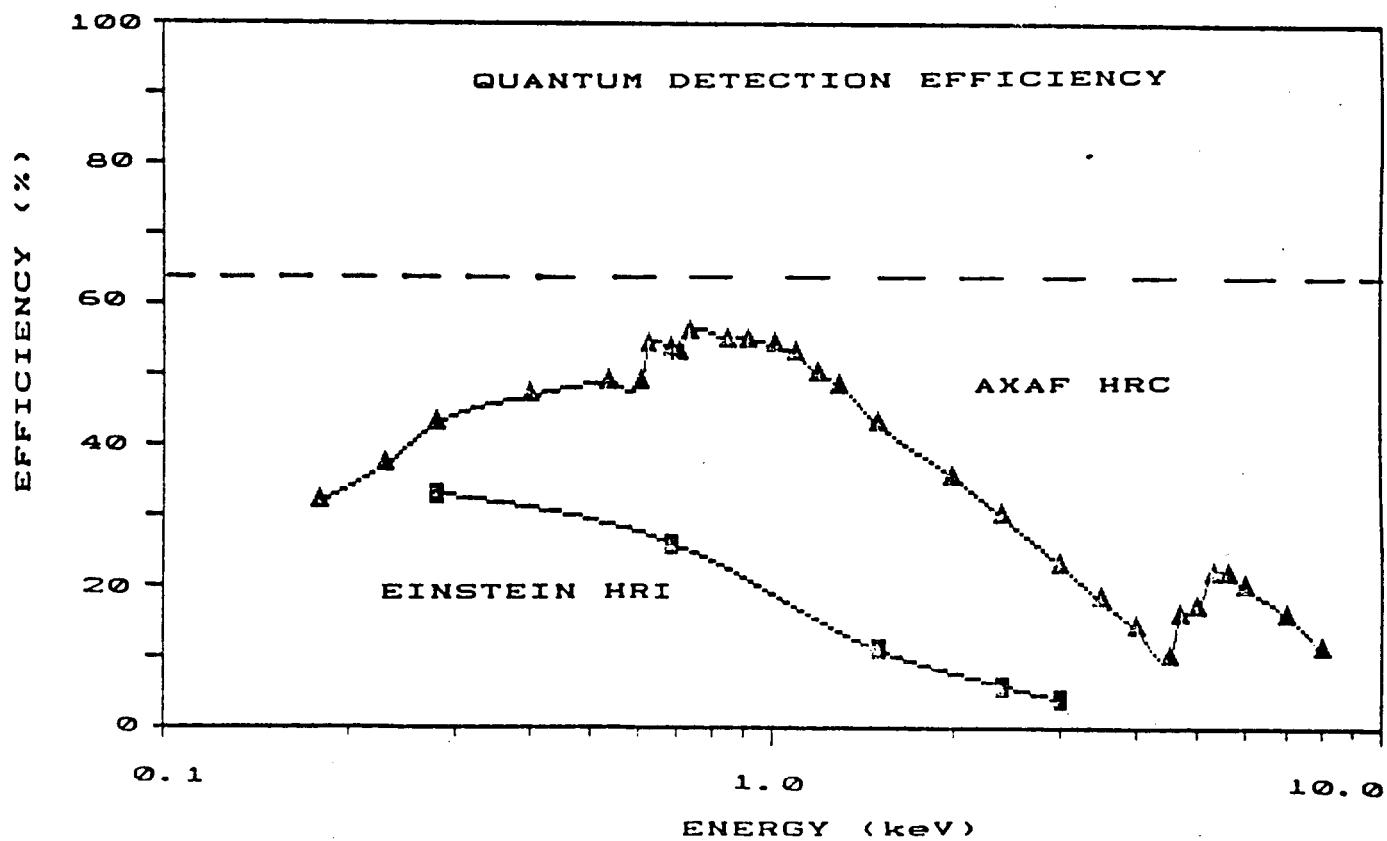


Figure 2

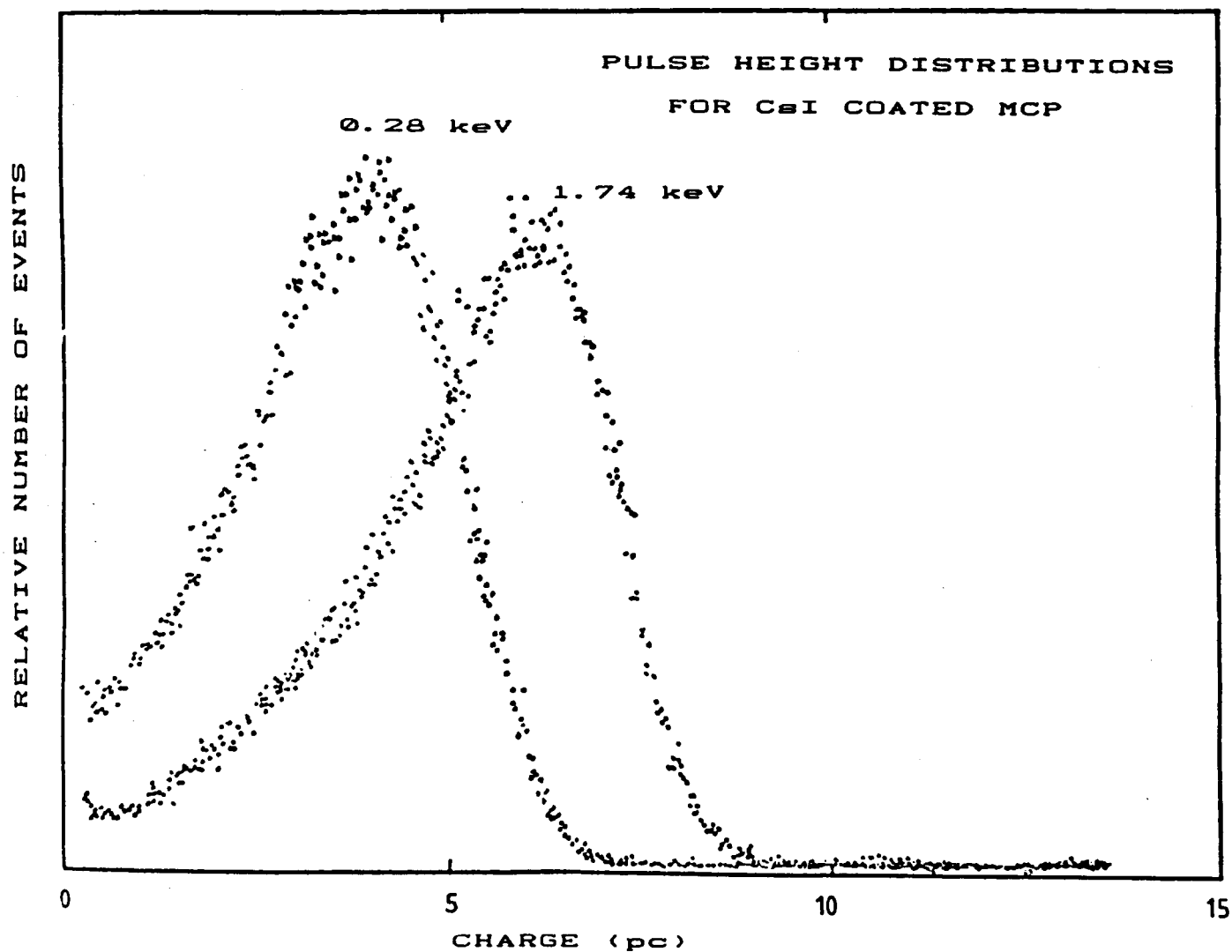


Figure 3

ORIGINAL PAGE IS
OF POOR QUALITY

= ||| = ||

= |||

HEAO-B

||| =

12.5 μ m open25 μ m open75 μ m closed

= |||

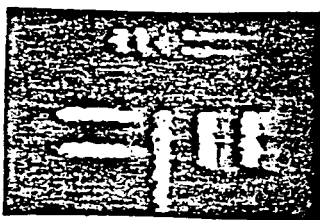
37.5 μ m closedFWHM = 25 μ m
(σ = 10.5 μ m)

Figure 4

SENSITIVITY 5 SIGMA FLUX MEASUREMENT

Power Law 1.4 NH 3E20

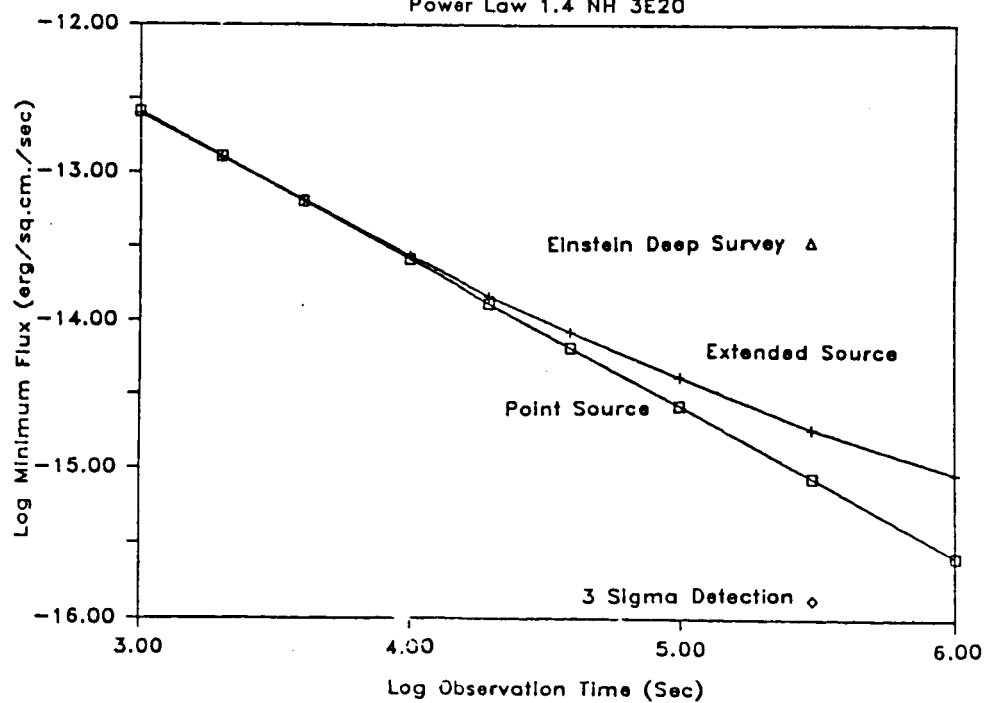


Figure 5

III. Phase B Statement of Work

TASK 1 - HRC Design

Carry out limited design studies sufficient to support the development of the Phase C/D cost and schedule preparation. Detailed designs to be deferred to Phase C/D. Provide preliminary estimates for weight, power, data, and command requirements of the HRC consistent with the configurations developed by the Facility definition contractors.

Mechanical Design Definition

Defer detailed design of the UV Cal source optics and mask until Phase C/D.

Processing Electronics Definition

Emphasize preamplifier design and packaging. Subcontract packaging studies to AS&E for all of the electronics to establish baselines needed for preparation of the Phase C/D proposal.

Support and Interface Structure Definition

Defer the preparation of Fracture Control Plan to Phase C/D. Defer the detailed structures design study until a single spacecraft contractor has been selected to avoid carrying out parallel efforts. Preliminary design work will be done to insure compatibility with both instrument accommodation approaches.

Electronic Interface Design

To avoid wasted effort in detailed design prior to the selection of a spacecraft contractor, we will assume an interface that can be accommodated by either contractor in establishing the preliminary design.

Detailed Definition for Aspect Determination Issues

Defer work in the general aspect determination area until Phase C/D. Concentrate Phase B efforts in the design of the fiducial light system and, in particular, the definition and location of the fiducial lights in the HRC.

Mechanical Ground Support Equipment Definition

Carry out definition studies sufficient for the preparation of the Phase C/D proposal.

Electronical Ground Support Equipment Definition

Carry out definition studies sufficient for the preparation of the Phase C/D proposal.

TASK 2 - BREADBOARD STUDIES

The modest material budget for the Definition Study indicates that work is well along and that most of the materials are in hand. Specifically, one set of 100mm x 100mm MCPs is already on hand, along with a 75mm x 75mm Cross Grid Charge Detector (CGCD), which is adequate to evaluate the MCP. Much of the background or preliminary testing is already complete. More testing will be required and some of the "trades" may well have been completed and we will be able to concentrate on a particular approach. Nonetheless, at this writing there are a few areas requiring some experimental work. These are:

- o continued evaluation of 100mm x 100mm MCPs
- o UV/Ion shield window support schemes
- o CsI photocathode configuration
- o anti-coincidence shield

Work related to MCP evaluation involves tests of the large area units and comparison of the Mullard MCP's with other units. It also involves deposition of CsI photocathodes and subsequent evaluation. CsI deposition on MCPs is provided both in the Definition and C/D Phases by both SAO and the University of Leicester. Most tests will be performed at SAO.

UV/Ion shields using both high transmission meshes and thin stretched polypropylene films will be constructed, evaluated, and traded. This work will be performed at SAO and University of Hawaii.

Some experimental work will be carried out to ensure that no problems arise due to the incorporation of the anti-coincidence scintillating shield inside the detector volume. The objective is to ensure material compatibility and effective optical coupling to the PMT.

Plastic will be purchased and a test shield and dummy housing wall will be constructed. The plastic will be coated and evaluated for outgassing. Brassboard PMT assemblies will be coupled to the plastic through the dummy wall and evaluated for thermal and mechanical stability. Pumping characteristics of the concept where the PMT penetrates the vacuum wall will be evaluated. This work will be carried out jointly by SAO and AS&E.

TASK 3 - PREPARATION OF UPDATED PROPOSAL

The output of this activity is a complete technical, cost, and management proposal which demonstrates the maturity of the instrument design and its compatibility with the AXAF Observatory. The proposal also supports cost and schedule plans in sufficient detail to demonstrate that development can begin with minimum cost/schedule risk to the program.

This activity is taken to include all of the planning and estimation which the proposal documents. It also includes the

development of plan outlines for Safety, Fracture Control, and Product Assurance, which will be included in the updated proposal. Detailed plans/requirements for Flight Operations and Data Reduction and Analysis will also be developed as part of this activity.

SAO will prepare a Statement of Work for the American Science and Engineering, Inc., portion of the development activity. AS&E will provide a complete and detailed proposal which will be incorporated by reference and appended to the SAO Phase C/D proposal.

Funding to AS&E under the contemplated Design Definition Support contract will be for definition studies and will require limited deliverable reports and drawings.

TASK 4

Limited support will be provided within the level of effort available to the IPI. Establishment of requirements and definitions will be supported, development of detailed plans will be limited by the available resources.

TASK 5 - PLANNING

Development of detailed planning techniques will be minimized in Phase B. This includes detailed WBS for Phase B, detailed task descriptions, task matrices, etc.